Design and Manufacturing of a Low-Profile Coaxial-to-Dual Ridge Waveguide Adapter for CubeSat Reflectarray Antenna Systems

Mustafa Murat Bilgic, Tonny Rubæk, Oscar Borries, Min Zhou

TICRA, Copenhagen, 1117, Denmark

***Abstract* — This work presents the design and manufacturing of a low-profile coaxial-to-dual ridge waveguide adapter operating in the X band from 8.025 GHz to 8.4 GHz. The adapter will connect the feed of the antenna system to the RF front-end. The antenna system is a polarizing reflectarray that has been designed as a downlink antenna for 6U CubeSat platforms. The tolerances necessary for the mechanical design were determined based on a detailed uncertainty quantification analysis such that the complete feed performance has minimal degradation against manufacturing tolerances. Measurement results are presented for comparison with the uncertainty quantification analysis.**

***Index Terms* — Uncertainty quantification, coaxial to waveguide adapters, reflectarray antennas, CubeSat antennas, waveguide components, antenna sub-systems.**

I. Introduction

CubeSats are promising candidates for a variety of space missions, due to their relatively low cost and short development times. However, the limited space available in a CubeSat makes it challenging to embark high-gain antennas on the platform. Such high-gain antennas are required for high-speed communication links and for microwave instruments requiring a narrow beamwidth, e.g., radiometers and radars. The antenna solutions available today are typically based on deployable reflector technology, e.g. [1], but this type of antenna will typically occupy 1-2 units of area to allow it to be stowed during launch.

The use of a planar reflectarray has been demonstrated in space, where a narrow-band high-gain X-band antenna was used to achieve data downlink from Mars [2]. The use of a planar reflectarray is also considered for future ESA missions, e.g. [3] and [4]. The main goal in the design of an antenna system suitable for these missions was to have a high-gain antenna that left the internal volume of the CubeSat fully useable for the mission payload.

An antenna system capable of satisfying the requirements defined by ESA for the two missions [3], [4] has been designed and reported in [5] – [7], the antenna system on a 6U CubeSat platform can be seen in Fig. 1. In the first phases of the design, the antenna system and its feed have been designed to have an extremely low profile when stored, leaving the CubeSat inner volume empty. However, the output of the feed was connected to a standard coaxial-to-dual ridge waveguide (DRWG) adapter during verification measurements of the antenna system. This standard adapter had a high profile of 26.5 mm which protruded into the valuable volume inside the CubeSat. To complete the antenna system, a low-profile coaxial-to-DRWG adapter is needed.

Fig. 1. Realized X-band polarizing reflectarray antenna system designed for 6U CubeSat platforms.

This paper is organized as the following. In Section II we provide a short overview of the polarizing reflectarray antenna system, which will be followed by a section describing the preliminary design of the low-profile coaxial-to-DRWG adapter in Section III. In Section IV, we cover the mechanical design of the adapter. The mechanical design is based on building a realizable mechanical model and running EM analysis to verify that the adapter will still meet the required performance. This is done by applying uncertainty quantification to the feed model using the commercially available UQ software product in TICRA Tools [8].

Finally, measurements of the reflection coefficient of the realized feed will be presented and compared with the outputs of the uncertainty quantification.

II. Overview of the Polarizing Reflectarray Antenna System

The reflectarray antenna system is a compact deployable reflectarray antenna operating in circular polarization (CP). It employs using three individual panels which measure approximately 33 x 20 cm^2 each. Each panel is realized as a symmetric sandwich structure with Rogers 4003C dielectric surrounding a fibre glass core. Fig 2. – 3. shows the stowed antenna system together with the deployment sequence.

The reflectarray antenna [5], where one combines uses of a polarizing reflectarray with a compact all-metallic feeding structure. The feeding structure provides [5] an incoming linearly polarized (LP) field, which is then converted by the reflectarray into a CP and highly focused beam in the far field. This concept allows the feed to be significantly simplified when compared to classic reflectarrays that requires a CP feed to provide a CP beam from the reflectarray. Fig 4. shows the reflectarray panels together with the PCB stack-up and geometry of the crossed-dipole unit cell.

The feed proposed here is based on a planar all-metallic cavity antenna which is flush mounted on the CubeSat body, implying that the RF connector is located inside the spacecraft and that the primary feed element does not need to deploy. The feed model is shown in Fig. 5.

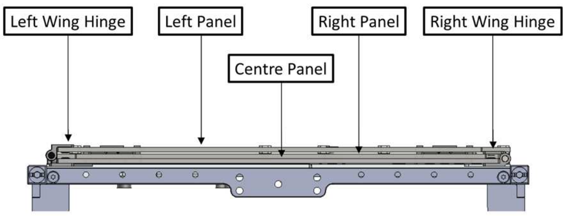

Fig. 2. CAD model of deployed antenna system.

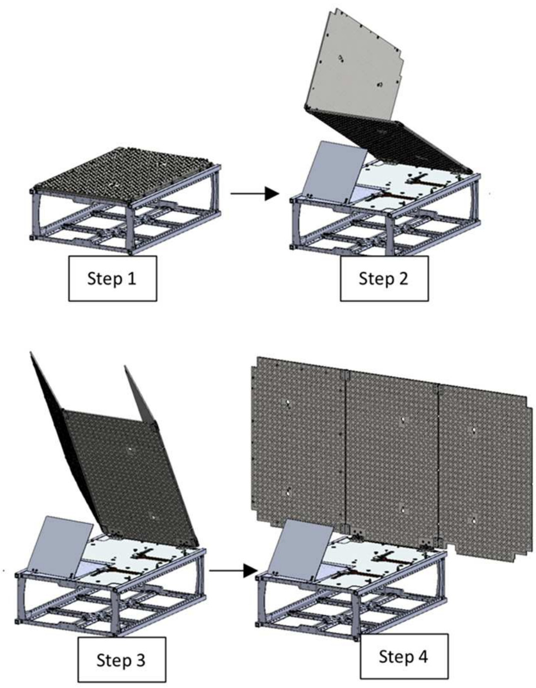

Fig. 2. Antenna system deployment sequence.

The radiation from the primary feed cavity is reoriented towards the reflectarray by a hinged aluminium plate acting as a small subreflector. The shape of the plate and the dimensions of the feed cavity have been carefully dimensioned to provide efficient illumination of the reflectarray while also maintaining a low return loss (>15dB) of the antenna system. This feeding arrangement is mechanically simple and low-loss, due to its all-metallic construction. As a further benefit, the primary feed is sufficiently compact for fitting into an existing recess in a standard CubeSat frame with no need for structural changes. The antenna provides a gain of approximately 29 dBi and the return loss at the waveguide port is better than 15 dB over the frequency range 8.025 GHz - 8.4 GHz, which covers the entire Earth observation downlink band. The complete antenna system shown in Fig. 3., has been modelled and optimised using TICRA Tools [8]. Further details regarding measurements and comparison to simulation results can be found in [6] - [7].

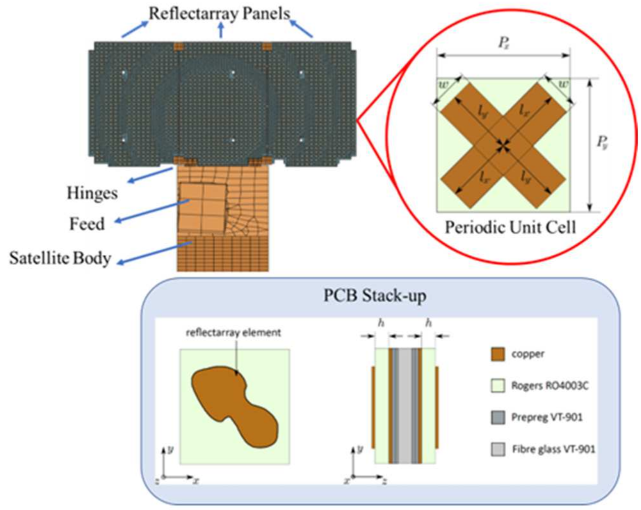

Fig. 4. Reflectarray antenna system model and periodic unit cell.

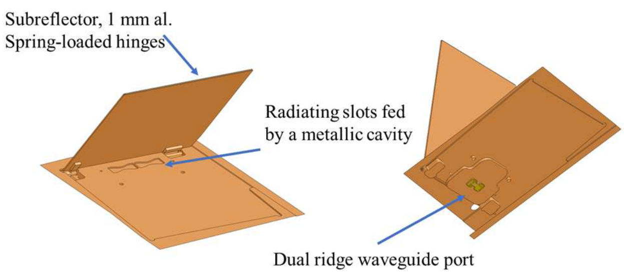

Fig. 5. Feed model of the cavity backed radiating slot antenna with planar subreflector.

III. Design of a Low-profile Coaxial-to-Dual ridge Waveguide Adapter

This section will describe the preliminary design of the low-profile coaxial-to-DRWG adapter. The basic block diagram for the proposed adapter is shown in Fig.6. The main goal of the adapter is to have a reflection coefficient less than -15 dB, and the adapter is desired to be all-metallic to reduce the losses. The adapter is built up of two 3-port power dividers, one having a dual ridge waveguide input port and one with a coaxial input port. The output ports of the power dividers have rectangular ports. One of these rectangular ports on each divider is terminated with short circuit. With the implementation of waveguide shorts, the power dividers have become DRWG/Coaxial – to – rectangular waveguide transitions. Then these two transitions are combined through a mode launcher and impedance matching device.

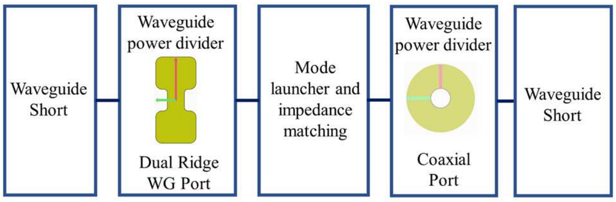

Fig. 6. Adapter topology block diagram.

The preliminary design steps start by tuning the power dividers such that input ports have a good impedance match and the output ports have equal power split; then by adding short circuit terminations to convert the power dividers to waveguide transitions. Then a final tunning is done to the dimensions of the intermediary transitions. Once the transitions are retuned, a suitable device which is the so called "mode launcher and impedance matching section" is added in between the two transitions, creating the complete adapter.

Fig. 7. shows the proposed adapter and Fig 8. shows the preliminary design results. The proposed adapter has two inputs, one DRWG and a coaxial port. The total height of the cavity is 3.56 mm.

An adapter that can achieve the specified reflection coefficient requires the mode launcher section to be specifically tailored. Gap waveguide structures are promising topologies for wideband low profile waveguide devices. The mode launcher in the proposed adapter uses a gap waveguide mode launcher similar to the one described in [9]. The model was built and optimized using the software CHAMP 3D available in TICRA Tools [8]. The parameters shown in Fig. 6, together with the height, width, and position of the bed of nails in the mode launcher, were the main optimization parameters.

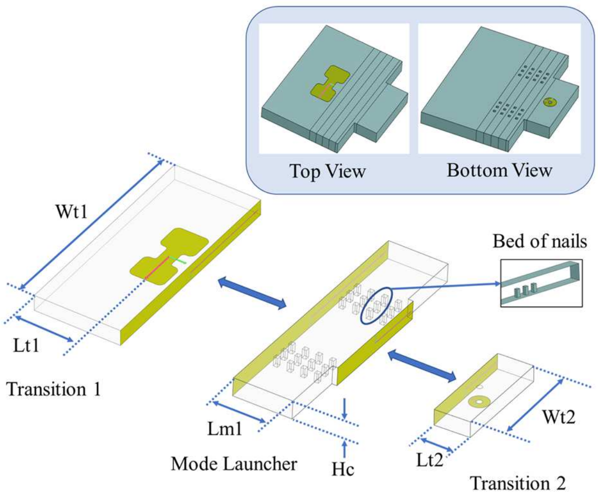

Fig. 7. Proposed adapter.

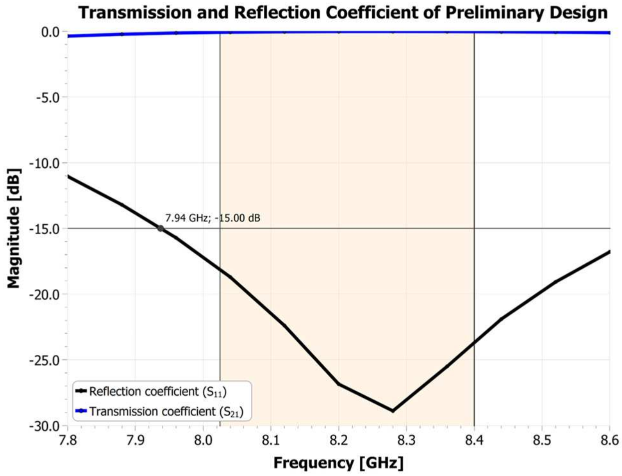

Fig. 8. Preliminary results of the proposed adapter.

Fig 8. shows the results for the preliminary design. It can be seen from the results that the preliminary design can satisfy the requirements for the desired low-profile transition.

IV. Mechanical Design and Determination of Tolerances using Uncertainty Quantification

No manufacturing method is capable of producing an item perfectly to the specified dimensions – there will always be a deviation, which is known as the tolerance. Setting tolerances for critical dimensions will ensure that the manufactured parts will result in a compliant device.

A common approach for obtaining these tolerances is to run some form of uncertainty quantification. However, general methods can be cumbersome to apply to complicated systems. In TICRA Tools [8], an Uncertainty Quantification (UQ) software is available, which allows the user to perform uncertainty quantification that uses methods based on higher-order approximations, such as Stochastic Collocation (SC) and Polynomial Chaos Expansion (PCE). These methods offer a better convergence rate for a moderate number of parameters [10] compared to the more commonly used Monte Carlo analysis.

Before determining the tolerances, we need to modify the adapter in the preliminary design such that it is suitable for manufacturing. This is done by rounding all sharp corners and introducing a tuning screw. The coaxial connector to be used in the realization will be a standard SMA connector. The main function for the tuning screw is to compensate for the tolerance of the coaxial centre pin height. Fig. 9. shows the modified design combined with the feed. A final optimization is made to tune the adapter.

Determining the tolerances may not be straight forward. However, the tighter the tolerances for a mechanical device are the higher the cost will be. There will also be increasing difficultly to manufacture. This is where uncertainty quantification plays an important role. For the sake of simplicity in understanding how the tolerances affect the performance, the variables are decoupled, and three separate uncertainty analyses are performed.

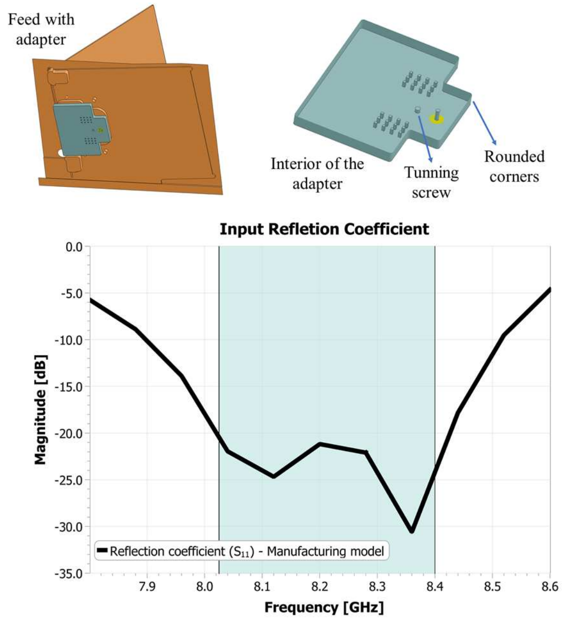

Fig. 9. Manufacturing model and input reflection coefficient after final optimization.

The three analysis groups are defined as follows:

- UQ1-Cavity dimensions: The lengths and widths of the adapter cavity. (Wt1, Wt2, Lt1, Lt2, Lm1 shown in Fig. 6.)
- UQ2-Bed of nails dimensions in mode launcher: Position, height, width, and inter-element spacings between the posts in the mode launcher.
- UQ3-Cavity and coaxial pin heights: The coaxial pin is not short circuited to the upper wall of the adapter cavity. The height of this pin and the height of the cavity are the most sensitive parameters for this device.

The uncertainty quantification analyses performed are all carried out using the SC method. The adapter is connected to the feed cavity (shown in Fig. 4.), and the overall performance of the feed assembly based on variations in the input variables are investigated. The feed has been proven to work as specified, so no parameters associated with the feed are included in the analyses. The tunning screw is also kept at its nominal position and not subject to uncertainty quantification.

The input variables used are assumed to have a uniform distribution. The output is the uncertainty of the reflection coefficient at the coaxial port within a confidence interval of 95%. The analyses are carried out for each frequency. A value, for which there is a 2.5% probability that the reflection coefficient is below, and another value, for which there is a 2.5% probability that the reflection coefficient is above, will be returned. The expected value of the reflection coefficient will also be returned.

For X-band applications, the UQ analyses shows that ±0.1 mm value for UQ1 and UQ2 are suitable, and the worst-case results still satisfy the -15 dB reflection coefficient specifications (see Fig. 10. - 11). However, ±0.1 mm is too high for UQ3. The highest tolerance value for cavity and coaxial pin heights that nearly satisfies the specifications is ±0.03 mm (See Fig. 12.). Reducing the tolerances more would increase the cost. A trade-off is made between cost and performance in a way that will affect the system minimally.

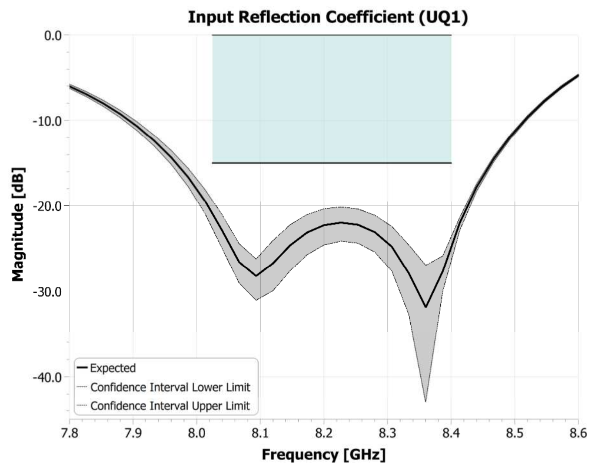

Fig. 10. Outputs with uncertainty for UQ1.

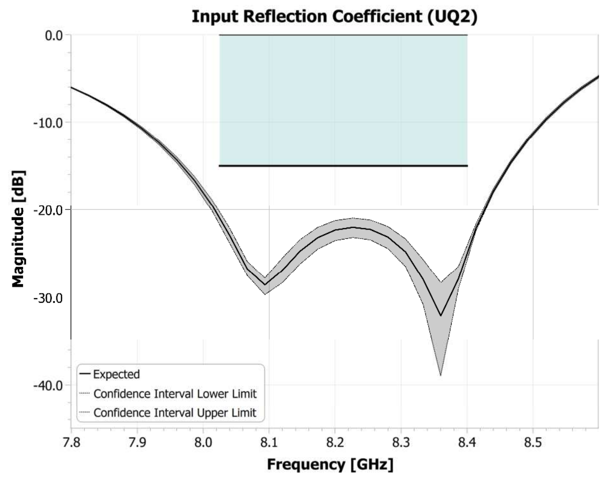

Fig. 11. Outputs with uncertainty for UQ2.

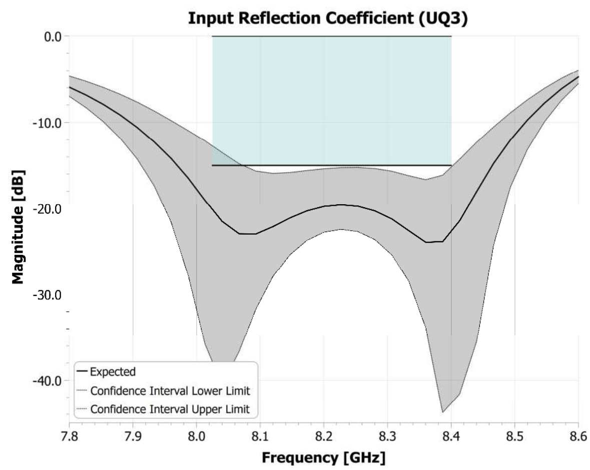

Fig. 12. Outputs with uncertainty for UQ3.

V. MEASUREMENTS AND COMPARISON WITH SIMULATIONS

The adapter has been manufactured according to the tolerances specified in the previous section. Fig. 13 shows the manufactured parts and the feed attached to the adapter on the right side. Three different samples have been manufactured and measurements have been carried out with a Keysight N9971A VNA. Measured input reflection coefficients for the three different adapters attached to the feed with the uncertainty quantification results achieved earlier can be seen in Fig. 14. For comparison, the three uncertainty quantification analysis results have been combined to include all uncertainty contributions into a single plot.

VI. CONCLUSION

The design and realization of a low-profile coaxial-to-dual ridge waveguide adapter have been presented. Using the UQ software in TICRA Tools, we were able to determine the tolerances necessary for manufacturing and predict the expected outcome when the device was manufactured and measured. The adapter has a return loss of more than 15 dB in the band from 8.025 GHz to 8.4 GHz. Adapter loss will be determined when the final gain measurements of the complete antenna system are completed. However, simulations estimate a loss around 0.2 dB.

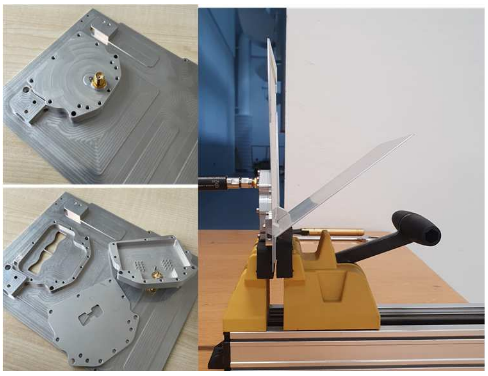

Fig. 13. Realized adapter.

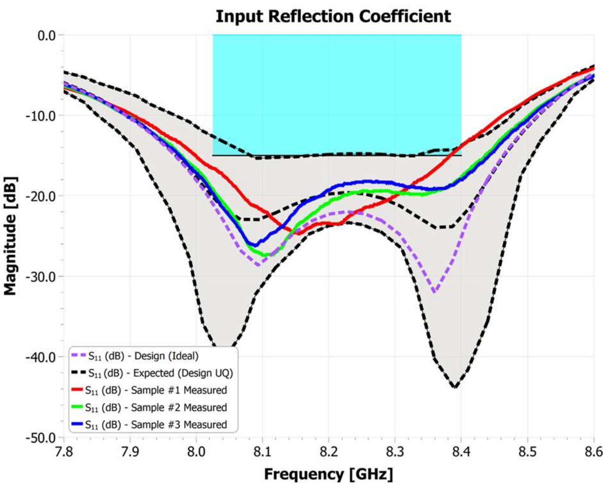

Fig. 14. Measured input reflection coefficients and calculated uncertainty intervals.

REFERENCES

[1] N. Chahat, R. E. Hodges, J. Sauder, M. Thomson, E. Peral, and Y. Rahmat-Samii, "Cubesat deployable Ka-band mesh reflector antenna development for earth science missions," *IEEE Trans. Antennas Propag*., vol. 64, no. 6, 2016.

[2] R. E. Hodges, N. Chahat, D. J. Hoppe, and J. D. Vacchione, "A deployable high-gain antenna bound for mars: Developing a new folded-panel reflectarray for the first cubesat mission to mars." *IEEE Antennas Propag. Mag*., vol. 59, no. 2, pp. 39–49, April 2017.

[3] C. B. R. Walker, D. Koschny and ESA CDF study team, "Miniaturised Asteroid Remote Geophysical Observer (MARGO)," *6th Interplanetary CubeSat Workshop, Cambridge*, UK, 2017.

[4] Gomspace, "GOMX-5 payload collaboration for the GOMX-5 mission," https://gomspace.com/news/payload-collaboration-initiated-for-the-gomx-.aspx, 2019.

[5] M. Zhou and E. Jørgensen, "Antenna system for satellite applications," *European Patent Application*, no. EP19176757.3, 2019

[6] E. Jørgensen, T. Rubæk, A. Ericsson, M. Zhou, J. B. Jensen, S. Christensen, E.L. Madsen, G. Toso and P. Maagt, "Development and Qualification of a high-gain X-band deployable reflectarray antenna for CubeSat applications," *40th ESA Antenna Workshop - Antenna Developments for Terrestrial and Small-Space Platforms*, October 2019

[7] T. Rubæk, M. Zhou, A. Ericsson, M.M. Bilgic and E. Jørgensen, "A reflectarray for CubeSat applications," *17th European Conference on Antennas and Propagation (EuCAP)*, Florance, Italy, 2023

[8] TICRA Tools User's Manual 22.1, TICRA, www.ticra.com.

[9] K. Ejiri, T. Tomura and J. Hirokawa, "Modal Analysis for Gap Waveguide Considering Structural Periodicity in Propagation Direction," *2019 International Symposium on Antennas and Propagation (ISAP)*, Xi'an, China, 2019, pp. 1-2.

[10] O. Borries, E. Jørgensen, P. Meincke, N. Vesterdal, M. F. Palvig and T. Rubæk, "Uncertainty quantification for reflector antennas," *12th European Conference on Antennas and Propagation (EuCAP 2018)*, 2018, pp. 1-5.